Design and Control of a Four-Wheeled Omnidirectional Mobile Robot with Steerable Omnidirectional Wheels

Jae-Bok Song and Kyung-Seok Byun
Department of Mechanical Engineering
Korea University
5, Anam-dong Sungbuk-gu
Seoul 136-701, Korea (South)
e-mail: jbsong@korea.ac.kr

Received 21 September 2003; accepted 27 December 2003

Omnidirectional mobile robots are capable of arbitrary motion in an arbitrary direction without changing the direction of wheels, because they can perform 3 degree-of-freedom (DOF) motion on a two-dimensional plane. In this research, a new class of omnidirectional mobile robot is proposed. Since it has synchronously steerable omnidirectional wheels, it is called an omnidirectional mobile robot with steerable omnidirectional wheels (OMR-SOW). It has 3 DOFs in motion and one DOF in steering. One steering DOF can function as a continuously variable transmission (CVT). CVT of the OMR-SOW increases the range of velocity ratio from the wheel velocities to robot velocity, which may improve performance of the mobile robot. The OMR-SOW with four omnidirectional wheels has been developed in this research. Kinematics and dynamics of this robot will be analyzed in detail. Various tests have been conducted to demonstrate the validity and feasibility of the proposed mechanism and control algorithm.

1. INTRODUCTION

Omnidirectional mobile robots are capable of moving in an arbitrary direction without changing the direction of wheels, because they can achieve 3 DOF motion on a two-dimensional plane. Various types of omnidirectional mobile robots have been proposed so far; universal wheels,[1,2] ball wheels,[3] and off-centered wheels[4] are popular among them.

Contract grant sponsor: Korea Research Foundation
Contract grant number: KRF-2003-041-D20038

The omnidirectional mobile robots using omnidirectional wheels composed of passive rollers or balls usually have three or four wheels. The three-wheeled omnidirectional mobile robots are capable of achieving 3 DOF motions by driving three independent actuators,[5,6] but they may have stability problems due to the triangular contact area with the ground, especially when traveling on a ramp with the high center of gravity owing to the payload they carry. It is desirable, therefore, that four-wheeled vehicles be used when stability is of great concern.[7] However,

independent drive of four wheels creates one extra DOF. To cope with such a redundancy problem, the mechanism capable of driving four omnidirectional wheels using three actuators was suggested.[8]

Another approach to a redundant DOF is to devise some mechanism which uses this redundancy to change wheel arrangements.[9,10] It is called a variable footprint mechanism (VFM). Since the relationship between the robot velocity and the wheel velocities depends on wheel arrangement, varying wheel arrangement can function as a transmission. Furthermore, it can be considered as a continuously variable transmission (CVT), because the robot velocity can change continuously by adjustment of wheel arrangements without employing a gear train. The CVT is useful to most mobile robots which have electric motors as actuators and a battery as a power source. Energy efficiency is of great importance in mobile robots because it is directly related to the operating time without recharging. Some mobile robots are equipped with a transmission system, but most mobile robots use gear trains with a fixed gear ratio because the transmission is heavy, bulky, and expensive. Therefore, transmission based on wheel arrangement provides the possibility of energy efficient drive. The CVT can provide more efficient motor driving capability as its range of velocity ratio gets wider. The mobile robot proposed by Wada,[9] however, has a limited range to ensure stability of the vehicle.

In this paper, an omnidirectional mobile robot with steerable omnidirectional wheels (OMR-SOW) is proposed to improve CVT performance in which robot stability is guaranteed regardless of wheel arrangement and thus the range of velocity ratio is greatly extended. The OMR-SOW is an omnidirectional mobile robot with 3 DOF motion and 1 DOF in steering. The steering DOF can be achieved by synchronously steerable omnidirectional wheels. While the VFM has a common steering axis for all four wheels, the OMR-SOW has an independent steering axis for each wheel. Therefore, the OMR-SOW possesses a wider range of velocity ratio without stability degradation. The four-wheeled omnidirectional mobile robot involving this mechanism combined with the continuous alternate wheels developed in our laboratory[11] has been developed.

The remainder of this paper is organized as follows. In Section 2, the structure of a variable wheel arrangement mechanism is introduced and the kinematics and dynamics of the OMR-SOW are presented. Section 3 explains how the CVT function is achieved in the OMR-SOW. Section 4 discusses construction of the OMR-SOW, its motion control, and some experimental results. Conclusions are drawn in Section 5.

2. OMNIDIRECTIONAL MOBILE ROBOT WITH STEERABLE OMNIDIRECTIONAL WHEELS

In this section, a new type of omnidirectional mobile robot, an omnidirectional mobile robot with steerable omnidirectional wheels (OMR-SOW), is introduced. Since four wheels of a robot can be independently driven, the OMR-SOW is of 4 DOFs: 2 DOFs for translation, 1 DOF rotation, and 1 DOF for steering. The steering DOF can function as a continuously variable transmission (CVT). In what follows, steerable omnidirectional wheels are introduced and the features of the OMR-SOW are discussed in detail.

2.1. Steerable Omnidirectional Wheels

Campion[12] classified nontrivial wheeled mobile robots into five categories according to degree of mobility and degree of steerability. He did not mention steerable omnidirectional wheels since most omnidirectional wheels did not have steering capability. However, steerable omnidirectional wheels have an additional DOF which can be used as a continuously variable transmission.

An omnidirectional wheel has 3 DOFs composed of wheel rotation, roller rotation, and rotational slip about the vertical axis passing through the point of contact.[7] Figure 1 shows a typical omnidirectional wheel in which the roller axes have an inclination angle γ with the wheel plane. Note that the wheel shown in the figure represents a general omnidirectional wheel and several different wheel mechanisms are available depending on roller types and inclination angles (e.g., universal wheel[1] with $\gamma = 0°$ and Mecanum wheel[2] with $\gamma = 45°$) In the omnidirectional wheel, the wheel velocity can be divided into the components in the active direction and in the passive direction. The active component is directed along the axis of the roller in contact with the ground, while the passive one is perpendicular to the roller axis.

In most cases omnidirectional wheels are fixed relative to the robot body and do not rotate for steering since steering can be performed by a combination of wheel velocities in these types of mechanisms. Omnidirectional wheels, however, are able to be combined with the steering mechanism as shown in Figure 2. Since the steering mechanism provides an additional DOF, this type of steerable

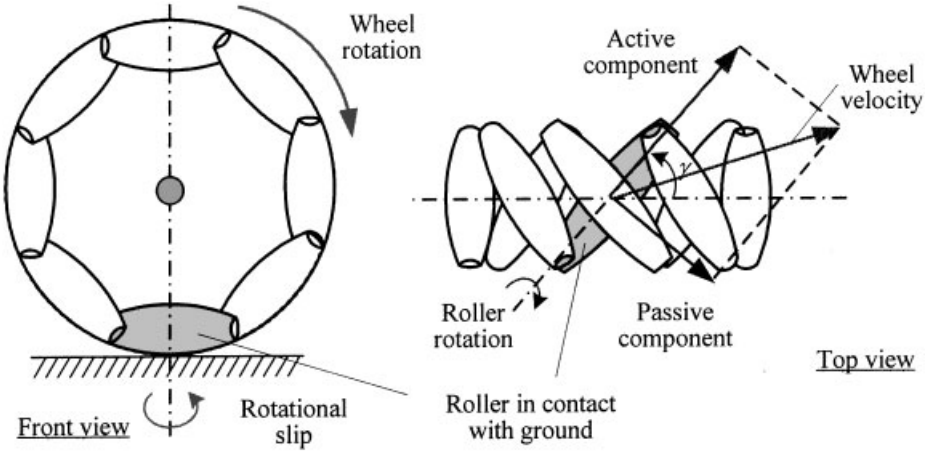

Figure 1. DOFs in a general omnidirectional wheel.

omnidirectional wheel module has one more DOF in addition to 3 DOFs defined in Figure 1. In Figure 2, the origin o represents the center of a robot and C the steering axis for the wheel shown. In the figure, ϕ is the steering angle, l is the offset distance, L_0 is the distance from the robot center to steering axis, and γ is the angle between the roller axis and the wheel plane, respectively.

As mentioned earlier, a steerable omnidirectional wheel has 4 DOFs. Since roller rotation and rotational slip do not impose any constraint on the wheel motion, the constraints can be obtained by the relationship between the robot velocity and the active wheel velocity (i.e., wheel velocity in the active direction). The active wheel velocity is given by

$$v_w = R\omega\cos\gamma, \tag{1}$$

where R is the wheel radius and ω is the angular velocity of a wheel.

Let the robot velocity vector be given as $\mathbf{V}_r = [v_x, v_y, \dot{\psi}, \dot{\phi}]^T$, where v_x and v_y are the translational velocities of the robot center, $\dot{\psi}$ is the angular velocity about the robot center, and $\dot{\phi}$ is the derivative of the steering angle, respectively. As shown in Figure 3, the active wheel velocity for a given robot velocity vector can be described by

$$v_{wx} = -v_x\cos(\theta-\phi-\gamma),$$

$$v_{wy} = v_y\sin(\theta-\phi-\gamma),$$

$$v_{w\psi} = \dot{\psi}\{l\cos\gamma + L_0\cos(\gamma+\phi)\},$$

$$v_{w\phi} = l\dot{\phi}\cos\gamma, \tag{2}$$

where v_{wx}, v_{wy}, $v_{w\psi}$, and $v_{w\phi}$ represent contribution of each component of the robot velocity vector to the active wheel velocity. The active wheel velocity is then obtained by summing these contributions up as follows:

$$v_w = v_{wx} + v_{wy} + v_{w\psi} + v_{w\phi}. \tag{3}$$

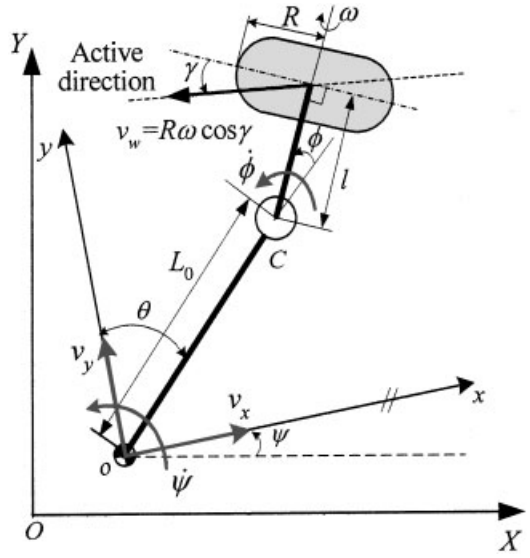

Figure 2. Coordinate systems and parameters for steerable omnidirectional wheel.

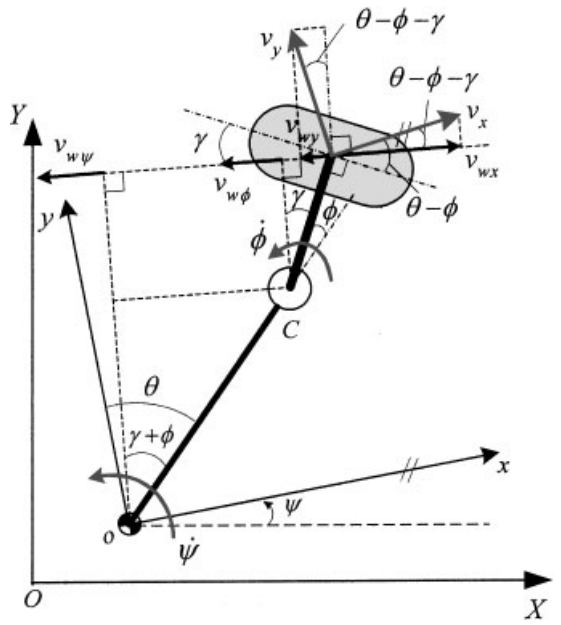

Figure 3. Geometric relations for deriving active wheel velocity.

Therefore, the constraint for a steerable omnidirectional wheel is described by

$$v_w = R\omega\cos\gamma = -v_x\cos(\theta-\phi-\gamma)+v_y\sin(\theta-\phi-\gamma) + \dot{\psi}(l\cos\gamma+L_0\cos(\gamma+\phi))+l\dot{\phi}\cos\gamma. \quad (4)$$

In the case of no offset (i.e., $l=0$), the constraint becomes

$$R\omega\cos\gamma = -v_x\cos(\theta-\phi-\gamma)+v_y\sin(\theta-\phi-\gamma) + \dot{\psi}L_0\cos(\gamma+\phi), \quad (5)$$

and in the case of $\gamma=0$, the constraint becomes

$$R\omega = -v_x\cos(\theta-\phi)+v_y\sin(\theta-\phi)+\dot{\psi}(l+L_0\cos(\phi)) + l\dot{\phi}. \quad (6)$$

If the velocity of a robot is given, the velocity of each wheel can obtained from Eq. (4) as a function of steering angle by

$$\psi = f(\phi) = [-v_x\cos(\theta-\phi-\gamma)+v_y\sin(\theta-\phi-\gamma) + \dot{\psi}\{l\cos\gamma+L_0\cos(\gamma+\phi)\}+l\dot{\phi}\cos\gamma]/(R\cos\gamma). \quad (7)$$

Note that a change in steering angle causes the relationship between the robot velocity and the wheel velocities to change, which enables a steerable omnidirectional wheel mechanism to function as a CVT.

On the other hand, Figure 4 shows the continuous alternate wheel (CAW) which was developed in our laboratory as an omnidirectional wheel. Note that this wheel has the same feature as a general omnidirectional wheel shown in Figure 1, except for an inclination angle $\gamma=0°$. Many types of omnidirectional wheels with passive rollers have gaps between rollers. Since these gaps cause a wheel to make

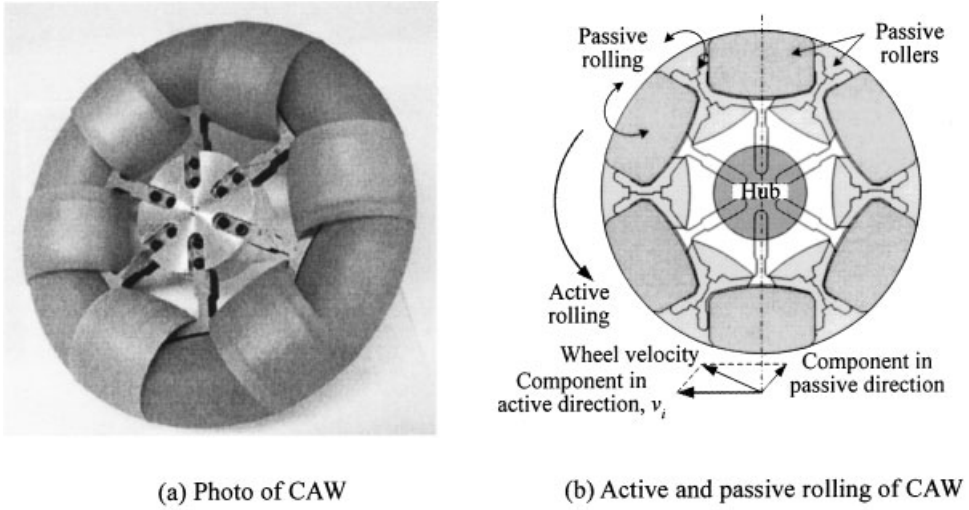

Figure 4. Appearance of continuous alternate wheel (CAW) and active and passive rolling.

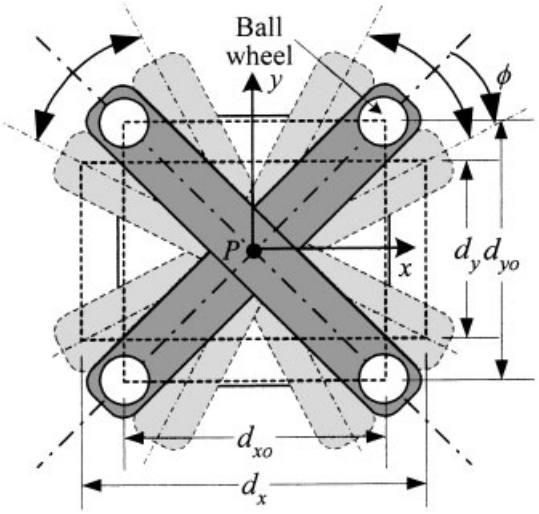

Figure 5. Variable footprint mechanism (VFM).

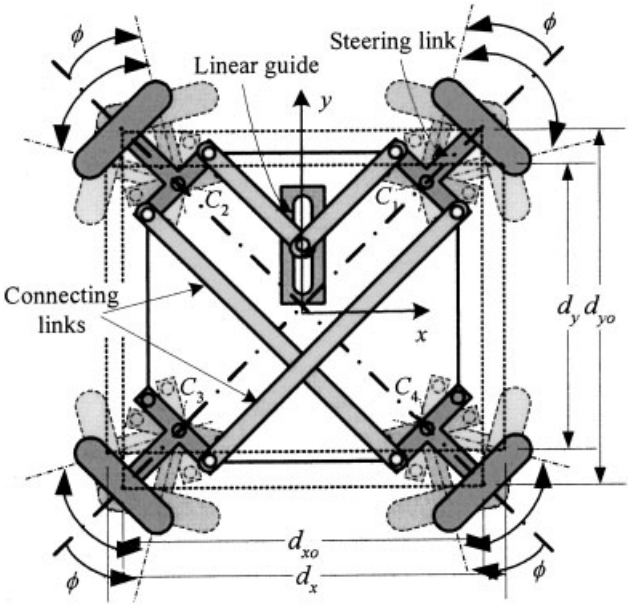

Figure 6. Variable wheel arrangement mechanism (VWAM) of OMR-SOW.

discontinuous contact with the ground, they lead to vertical and/or horizontal vibrations during wheel operation. However, the CAW makes continuous contact with the ground with alternating large and small rollers around the wheel, so virtually no vibration is created during operation.

2.2. OMR-SOW with Four Offset Steerable Omnidirectional Wheels

In this section, the structure and operational principle of the proposed OMR-SOW will be presented. In addition, detailed comparison of this mechanism with the variable footprint mechanism (VFM) proposed by Wada and Asada[9,10] will be discussed below.

Figure 5 shows the variable footprint mechanism (VFM) in which two beams can rotate at a pivot joint P in the middle. Note that the two beams are constrained to rotate in a symmetric fashion with a single DOF by means of differential gears at the pivot. The ball wheels and motors are mounted at each end of the beams. Meanwhile, the OMR-SOW developed in this research is illustrated in Figure 6. Notice that the four wheel modules can rotate about each pivot point $C_1,\ldots,C_4$ located at the corners of the robot body, but they are constrained to have a synchronized steering motion of 1 DOF by the synchronous mechanism comprising a linear guide and connecting links.

In Figures 5 and 6, the steering angle ϕ is defined as the angle from the zero position in which the beams (Figure 5) or the lines (i.e., C_1C_3 or C_2C_4) connecting the centers of diagonally opposed wheels (Figure 6) coincide with the diagonal lines of the robot body. The wheelbases, the distances between the centers of two adjacent wheels on the x- and y-axis, at the configuration $\phi=0$ are denoted as d_{xo} and d_{yo}. If the robot body is square, then $d_{xo}=d_{yo}$.

In Figure 5 the rotation center of the wheel module is located at the intersection P of the two beams. As the steering angle ϕ becomes large, therefore, one side of the rectangle whose vertices are wheel-to-ground contact points may get excessively smaller than the other side, thus leading to a significant decrease in tipping stability. Hence the steering angle was limited to the range between −17.5° and +17.5°, which causes the range of velocity ratio (defined in Section 3.1) to be limited. On the contrary, since the wheel modules in Figure 6 rotate about each pivot joint $C_1,\ldots,C_4$ placed at the corners of a robot platform, the robot is structurally stable even for a large steering angle. As a result of this feature, the steering angle can be substantially large, and thus the range of velocity ratio increases accordingly. Figure 7 shows various wheel arrangements.

Let us define the wheelbase ratio as follows:

$$r_{wb}=\frac{\min(d_x,d_y)}{d_{xo}}, \tag{8}$$

where d_x and d_y represent the wheelbase (i.e., the distance between the wheel centers) in the x and y directions as shown in Figures 5 and 6. Figure 8

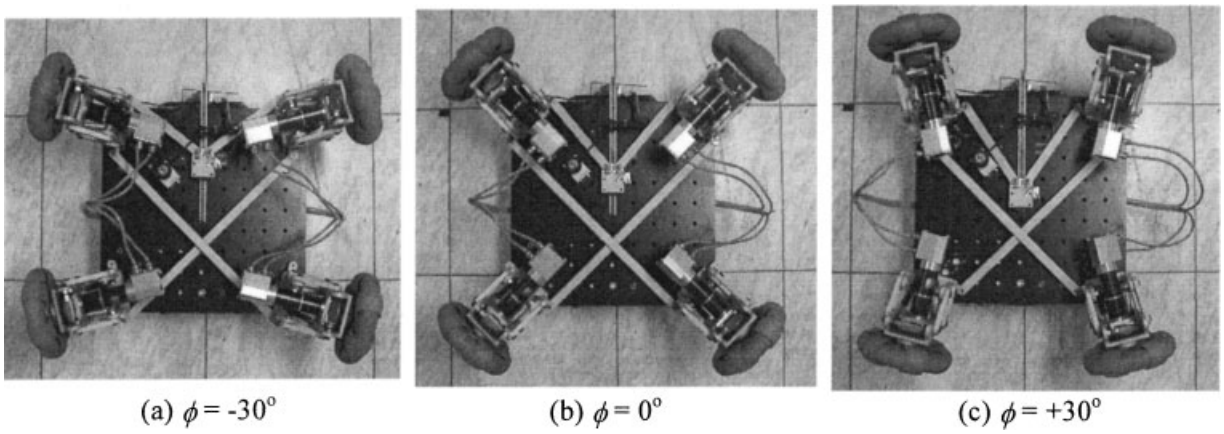

Figure 7. Various wheel arrangements of OMR-SOW.

illustrates the wheelbase ratios for the two mechanisms as a function of the steering angle. As shown in the figure, the proposed variable wheel arrangement mechanism provides a much wider range of steering angle without degrading tipping stability, since the change in r_{wb} is smaller than that for the variable footprint mechanism.

2.3. Kinematic Analysis of OMR-SOW

The four-wheeled omnidirectional mobile robot is illustrated in Figure 9. This schematic is a simplified version of the OMR-SOW in Figure 6 for convenience, which yields the same kinematic analysis as the mechanism in Figure 6. The frame *O-XY* is assigned as a reference frame for the robot motion in the plane and the moving frame *o-xy* is attached to the robot center. On the other hand, the angle θ between the *y*-axis and the diagonal line of the robot platform depends on the shape of a platform (i.e., $\theta = 45°$ for the square platform).

Using Eq. (6), the relationship between the wheel velocity vector and the vehicle velocity vector can be given by

$$\begin{Bmatrix} v_1 \\ v_2 \\ v_3 \\ v_4 \end{Bmatrix} = \begin{bmatrix} -C & S & L & l \\ -C & -S & L & -l \\ C & -S & L & l \\ C & S & L & -l \end{bmatrix} \begin{Bmatrix} v_x \\ v_y \\ \dot{\psi} \\ \dot{\phi} \end{Bmatrix}, \tag{9}$$

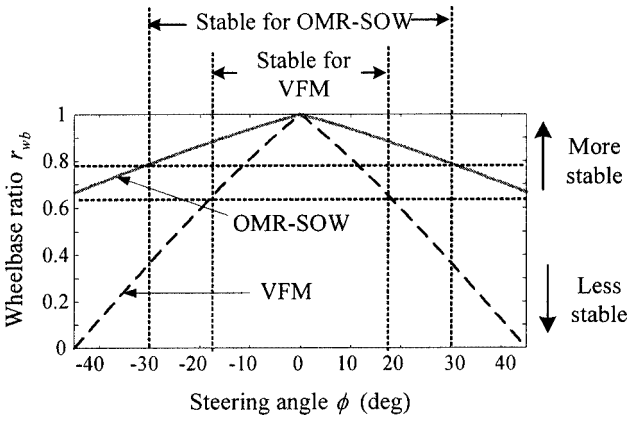

Figure 8. Comparison of wheelbase ratios for OMR-SOW and VFM.

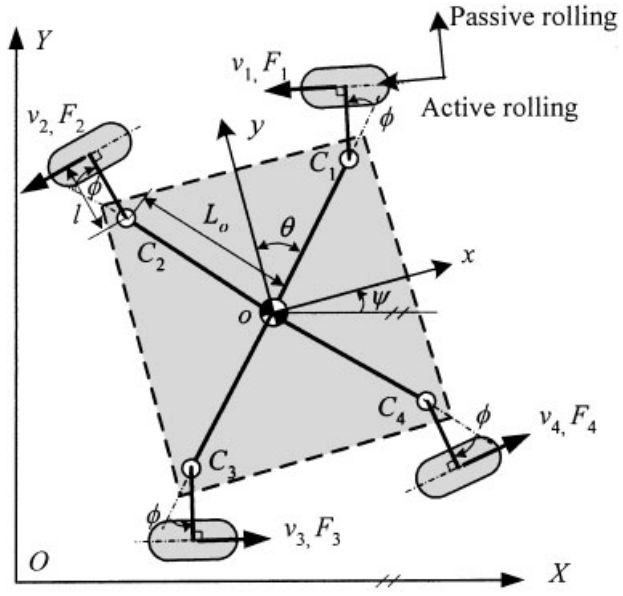

Figure 9. Coordinate systems for OMR-SOW under consideration.

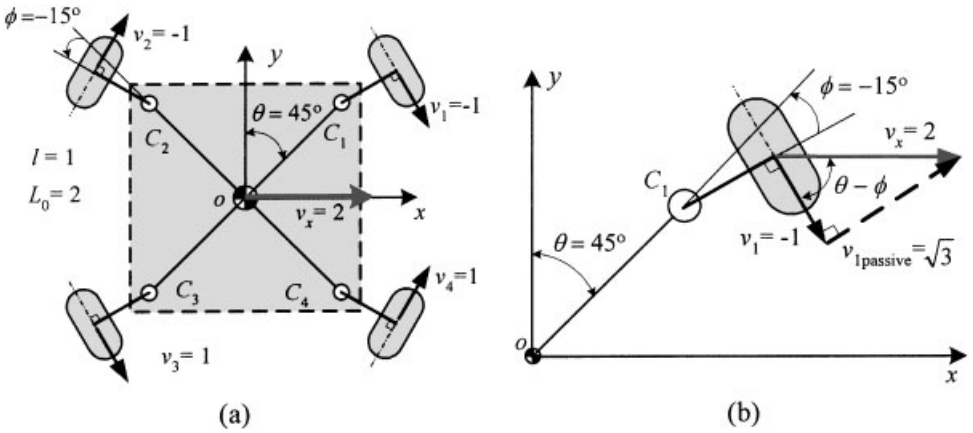

Figure 10. Example in kinematics.

where $C = \cos(\theta - \phi)$, $S = \sin(\theta - \phi)$, $L = L_o \cos\phi + l$, and v_1, v_2, v_3, v_4 are the wheel velocities in the active direction. The matrix in Eq. (9) is invertible, since $C \neq 0$ and $S \neq 0$ for $0 < \theta - \phi < 90°$. The inverse matrix is obtained by

$$\mathbf{J} = \frac{1}{4}\begin{bmatrix} -1/C & -1/C & 1/C & 1/C \\ 1/S & -1/S & -1/S & 1/S \\ 1/L & 1/L & 1/L & 1/L \\ 1/l & -1/l & 1/l & -1/l \end{bmatrix}, \quad (10)$$

which corresponds to the Jacobian matrix relating the wheel velocity vector to the robot velocity vector as follows:

$$\mathbf{V}_w = \mathbf{J}^{-1}\mathbf{V}_r \quad \text{or} \quad \mathbf{V}_r = \mathbf{J}\mathbf{V}_w, \quad (11)$$

where $\mathbf{V}_w = [v_1 \;\; v_2 \;\; v_3 \;\; v_4]^T$ and $\mathbf{V}_r = [v_x \;\; v_y \;\; \dot{\psi} \;\; \dot{\phi}]^T$. It follows from Eq. (11) that the robot velocity and steering velocity of the OMR-SOW can be completely determined by control of four independent motors driving each wheel.

To help in understanding the operational principle of the OMR-SOW, let us consider the following example. Suppose that the parameters are $\theta = 45°$, $\phi = -15°$, $L_o = 2$, $l = 1$ as shown in Figure 10(a). If the robot velocity is given by $\mathbf{V}_r = [2 \;\; 0 \;\; 0 \;\; 0]^T$, C, S, and L become

$$C = \cos(45° + 15°) = \tfrac{1}{2},$$

$$S = \sin(45° + 15°) = 2/\sqrt{3}, \quad (12)$$

$$L = L_o \cos(-15°) + l = 2.932.$$

Then, Eq. (11) can be calculated as

$$\mathbf{V}_w = \mathbf{J}^{-1}\mathbf{V}_r,$$

$$\begin{Bmatrix} v_1 \\ v_2 \\ v_3 \\ v_4 \end{Bmatrix} = \begin{bmatrix} -1/2 & \sqrt{3}/2 & 2.932 & 1 \\ -1/2 & -\sqrt{3}/2 & 2.932 & -1 \\ 1/2 & -\sqrt{3}/2 & 2.932 & 1 \\ 1/2 & \sqrt{3}/2 & 2.932 & -1 \end{bmatrix} \begin{Bmatrix} 2 \\ 0 \\ 0 \\ 0 \end{Bmatrix} = \begin{Bmatrix} -1 \\ -1 \\ 1 \\ 1 \end{Bmatrix}. \quad (13)$$

Figure 10(a) shows the active wheel velocities to produce the desired robot velocity. Note that the desired robot velocity contains only the translational velocity in the x direction, so the resultant velocity of each wheel has the magnitude of 2 in the x direction. From this observation, it follows that the passive wheel velocity of wheel 1 has the magnitude of $\sqrt{3}$ to form the specified resultant wheel velocity as shown in Figure 10(b).

2.4. Dynamic Analysis of OMR-SOW

Consider the dynamic model of a robot shown in Figure 9. The robot motion on the fixed coordinate system XY is described by

$$\mathbf{M}_r \dot{\mathbf{V}}_R = \mathbf{F}_R, \quad (14)$$

where

$$\mathbf{M}_r = \begin{bmatrix} M & 0 & 0 & 0 \\ 0 & M & 0 & 0 \\ 0 & 0 & I_z & 0 \\ 0 & 0 & 0 & I_\phi \end{bmatrix},$$

$$\mathbf{V}_R = \begin{bmatrix} v_X \\ v_Y \\ \dot{\psi} \\ \dot{\phi} \end{bmatrix}, \quad \text{and} \quad \mathbf{F}_R = \begin{bmatrix} F_X \\ F_Y \\ T_Z \\ T_\phi \end{bmatrix},$$

where M is the mass of a robot, I_z is the moment of inertia about the z axis passing through the robot center and I_ϕ is the moment of inertia about the steering axis of the wheel modules. Note that the subscript R represents the fixed reference frame.

The transformation matrix from the moving robot frame $\{r\}$ to the fixed reference frame $\{R\}$ is given by

$$\mathbf{R} = \begin{bmatrix} \cos\psi & -\sin\psi & 0 & 0 \\ \sin\psi & \cos\psi & 0 & 0 \\ 0 & 0 & 1 & 0 \\ 0 & 0 & 0 & 1 \end{bmatrix}. \tag{15}$$

The relationship between the fixed reference frame and the moving robot frame is described by

$$\mathbf{V}_R = \mathbf{R}\cdot\mathbf{V}_r, \quad \mathbf{F}_R = \mathbf{R}\cdot\mathbf{F}_r. \tag{16}$$

Differentiation of $\mathbf{V}_R$ is given by

$$\dot{\mathbf{V}}_R = \mathbf{R}\dot{\mathbf{V}}_r + \dot{\mathbf{R}}\mathbf{V}_r. \tag{17}$$

Therefore, the robot of Eq. (14) is described on the moving coordinate system by

$$\mathbf{M}_r(\mathbf{R}\dot{\mathbf{V}}_r + \dot{\mathbf{R}}\mathbf{V}_r) = \mathbf{R}\mathbf{F}_r \quad \text{or} \quad \mathbf{R}^{-1}\mathbf{M}_r(\mathbf{R}\dot{\mathbf{V}}_r + \dot{\mathbf{R}}\mathbf{V}_r) = \mathbf{F}_r. \tag{18}$$

On the other hand, the force and moment of a robot can be expressed from the geometry in Figure 9 by

$$\begin{aligned} F_x &= -CF_1 - CF_2 + CF_3 + CF_4, \\ F_y &= SF_1 - SF_2 - SF_3 + SF_4, \\ T_z &= LF_1 + LF_2 + LF_3 + LF_4, \\ T_\phi &= lF_1 - lF_2 + lF_3 - lF_4, \end{aligned} \tag{19}$$

where F_x and F_y are the forces acting on the robot center in the x and y directions, T_z is the moment about the z axis passing through the robot center, and T_ϕ is the torque required to rotate the wheel modules, respectively. Note that the force $F_i (i = 1,...,4)$ is the traction force acting on the wheel in the direction of active rolling. Using the Jacobian matrix defined in Eq. (10), the relationship between the wheel traction forces and the resultant forces acting on the robot body is given by

$$\mathbf{F}_r = \mathbf{J}^{-T}\mathbf{F}_w \quad \text{or} \quad \mathbf{F}_w = \mathbf{J}^T\mathbf{F}_r, \tag{20}$$

where $\mathbf{F}_w = [F_1 \;\; F_2 \;\; F_3 \;\; F_4]^T$ and $\mathbf{F}_r = [F_x \;\; F_y \;\; T_z \;\; T_\phi]^T$. It is noted that $\mathbf{F}_r$ is given by a vectorial sum of traction forces. Varying a combination of the traction forces can generate arbitrary forces and moments for driving the vehicle and the moment for steering the wheel modules.

In addition, wheel forces are given by

$$R\mathbf{F}_w = \mathbf{U} - I_w\dot{\boldsymbol{\omega}}_w - c_w\boldsymbol{\omega}_w \quad \text{or} \quad R\mathbf{F}_w = \mathbf{U} - \frac{I_w}{R}\dot{\mathbf{V}}_w - \frac{c_w}{R}\mathbf{V}_w, \tag{21}$$

where R is the wheel radius, $\mathbf{U} = [u_1 \;\; u_2 \;\; u_3 \;\; u_4]^T$, where u_i is the motor torque of the ith motor, I_w is the moment of inertia of the wheel about the drive axis and c_w is the viscous friction factor of the wheel, and $\boldsymbol{\omega}_w = [\omega_1 \;\; \omega_2 \;\; \omega_3 \;\; \omega_4]^T$, where ω_i is the angular velocity of the ith wheel. From Eq. (11), the wheel velocity and acceleration vectors are obtained by

$$\begin{aligned} \mathbf{V}_w &= \mathbf{J}^{-1}\mathbf{V}_r, \\ \dot{\mathbf{V}}_w &= \dot{\mathbf{J}}^{-1}\mathbf{V}_r + \mathbf{J}^{-1}\dot{\mathbf{V}}_r. \end{aligned} \tag{22}$$

After substitution of Eqs. (20)–(22) into (18), the following relation is obtained:

$$\mathbf{R}^{-1}\mathbf{M}_r(\mathbf{R}\dot{\mathbf{V}}_r+\dot{\mathbf{R}}\mathbf{V}_r)=\mathbf{J}^{-T}\mathbf{F}_w$$
$$=\mathbf{J}^{-T}\frac{1}{R}\left(\mathbf{U}-\frac{I_w}{R}\dot{\mathbf{V}}_w-\frac{c_w}{R}\mathbf{V}_w\right)$$
$$=\mathbf{J}^{-T}\left(\frac{1}{R}\mathbf{U}-\frac{I_w}{R^2}\times(\dot{\mathbf{J}}^{-1}\mathbf{V}_r+\mathbf{J}^{-1}\dot{\mathbf{V}}_r)-\frac{c_w}{R^2}\mathbf{J}^{-1}\mathbf{V}_r\right). \quad (23)$$

This can be simplified by use of the relation $\mathbf{R}^{-1}\mathbf{M}_r\mathbf{R}=\mathbf{M}_r$ to

$$\left(R\mathbf{J}^T\mathbf{M}_r+\frac{I_w}{R}\mathbf{J}^{-1}\right)\dot{\mathbf{V}}_r+\left(R\mathbf{J}^T\mathbf{R}^{-1}\mathbf{M}_r\dot{\mathbf{R}}+\frac{I_w}{R}\dot{\mathbf{J}}^{-1}+\frac{c_w}{R}\mathbf{J}^{-1}\right)\mathbf{V}_r=\mathbf{U}. \quad (24)$$

Eq. (24) represents the dynamic model of a robot.

3. CVT OF OMR-SOW

As explained in Section 2, a change in the steering angle of the OMR-SOW functions as a CVT. In this section CVT of the OMR-SOW is discussed in detail.

3.1. Velocity and Force Ratios

Since the omnidirectional mobile robot has 3 DOFs in the 2-D plane, it is difficult to define the velocity ratio in terms of scalar velocities. Thus the velocity ratio is defined using the concept of norms as follows:

$$r_v=\frac{\|\mathbf{V}_r\|}{\|\mathbf{V}_w\|}=\frac{\|\mathbf{J}\mathbf{V}_w\|}{\|\mathbf{V}_w\|}. \quad (25)$$

Note that the velocity ratio for the identical wheel velocities varies depending on the steering angle. For example, suppose that a robot has a translational motion in the x axis. The robot velocity is then given by

$$\mathbf{V}_r=[1 \quad 0 \quad 0 \quad 0]^T. \quad (26)$$

From Eq. (11), the wheel velocity is computed as

$$\mathbf{V}_w=[-C \quad -C \quad C \quad C]^T. \quad (27)$$

From Eq. (25), the velocity ratio is obtained as

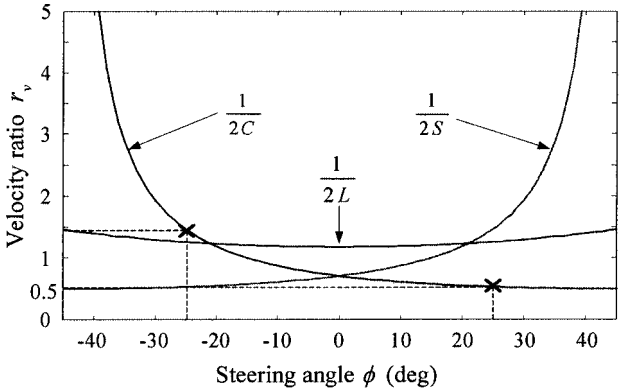

Figure 11. Velocity ratios as a function of steering angle.

$$r_v=\frac{1}{2C}=\frac{1}{2\cos(\theta-\phi)}. \quad (28)$$

Similarly, if a robot has a translational motion in the y axis (i.e., $\mathbf{V}_r=[0 \ 1 \ 0 \ 0]^T$), then the velocity ratio is given by

$$r_v=\frac{1}{2S}=\frac{1}{2\sin(\theta-\phi)}. \quad (29)$$

For rotational motion given by $\mathbf{V}_r=[0 \ 0 \ 1 \ 0]^T$, the velocity ratio is

$$r_v=\frac{1}{2L}=\frac{1}{2(L_0\cos\varphi+l)}. \quad (30)$$

Figure 11 shows the velocity ratio profiles as a function of steering angle in case of $L_o=0.283$ m, $l=0.19$ m, and $\theta=45°$. It is observed that the translational velocity ratios vary significantly in the range between 0.5 and infinity, while the rotational velocity ratio is kept nearly constant.

The velocity ratio is sensitive to translational motions. If the velocity direction of a robot is at α to the x-axis as shown in Figure 12, the robot velocity is given by

$$\mathbf{V}_r=[\cos a \quad \sin a \quad 0 \quad 0]^T. \quad (31)$$

The velocity ratio is then obtained as a function of steering angle and velocity direction

$$r_v=f(\phi,a). \quad (32)$$

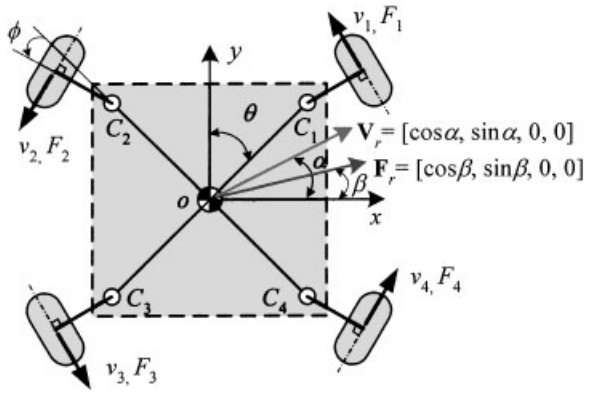

Figure 12. Velocity and force directions.

Figure 13 shows this relation. It is observed that the range of velocity ratio becomes wide as the steering angle grows in either sense.

The force ratio of the force acting on the robot center to the wheel traction force can be defined in the same way as the velocity ratio in Eq. (25):

$$r_f = \frac{\|\mathbf{F}_v\|}{\|\mathbf{F}_w\|} = \frac{\|\mathbf{J}^{-T}\mathbf{F}_w\|}{\|\mathbf{F}_w\|} = \frac{1}{r_v}. \tag{33}$$

Note that the force ratio corresponds to the inverse of the velocity ratio. Similar to the velocity ratio, if a robot has translational and rotational motions, the force ratio can be obtained as

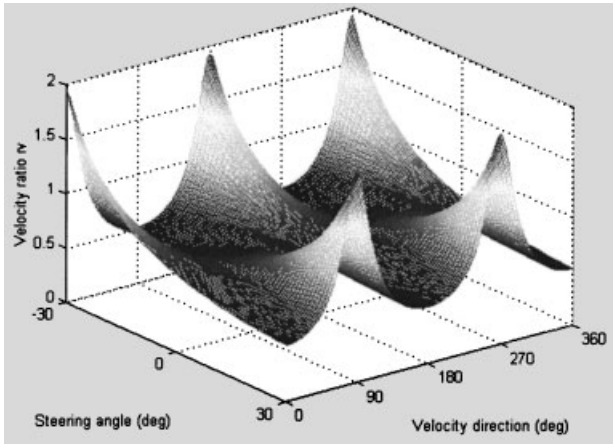

Figure 13. Velocity ratio as a function of steering angle and velocity direction.

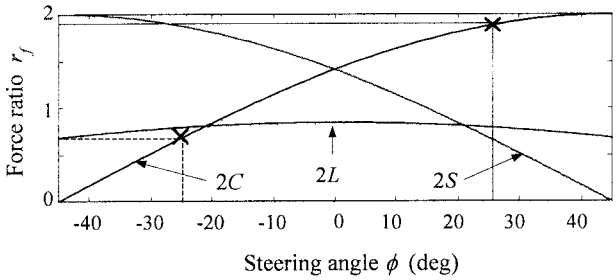

Figure 14. Force ratios as a function of steering angle.

$$r_f = 2\cos(\theta-\phi) = 2C \quad \text{for} \quad \mathbf{F}_r = [1 \quad 0 \quad 0 \quad 0]^T,$$

$$r_f = 2\sin(\theta-\phi) = 2S \quad \text{for} \quad \mathbf{F}_r = [0 \quad 1 \quad 0 \quad 0]^T,$$

$$r_f = 2(L_0\cos\phi + l) = 2L \quad \text{for} \quad \mathbf{F}_r = [0 \quad 0 \quad 1 \quad 0]^T. \tag{34}$$

Figure 14 shows the force ratio as a function of steering angle. It is observed that the force ratio becomes maximum in one direction, while minimum in the other direction as the steering angle reaches its maximum magnitude $\phi_{\max}$. Therefore, the steering angle should be determined so that the robot force to meet given specifications is generated.

Similar to the velocity case, if a robot has arbitrary force direction β, $\mathbf{F}_r = [\cos\beta \ \sin\beta \ 0 \ 0]^T$, as shown in Figure 12, the force ratio is given by

$$r_f = g(\phi,\beta) = \frac{1}{f(\phi,\beta)} = \frac{1}{r_v}. \tag{35}$$

3.2. Selection of Motors

A motor has an operating region in which continuous operation is guaranteed as shown in Figure 15. This region is delimited by various factors such as maximum permissible speed, maximum continuous torque, and power rating. Most motors have characteristics of low torques and high speeds, which corresponds to region I (*a-d-e-l*). Use of a speed reducer combined with the motor can modify the operating region to region II (*a-b-m-n-k-a*) by lowering speeds and amplifying torques. When a transmission device such as the CVT mechanism is added to the system, the operating region can be further extended to regions III (*a-c-f-i-j-a*).

Typical performance indices such as the maximum velocity, maximum acceleration, and

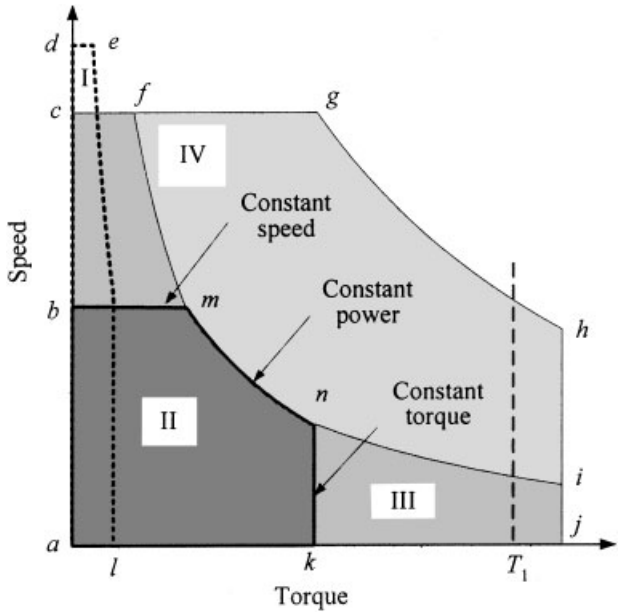

Figure 15. Operating regions of motor (I: motor, II: motor+speed reducer, III: motor+speed reducer+CVT, IV: large motor+speed reducer).

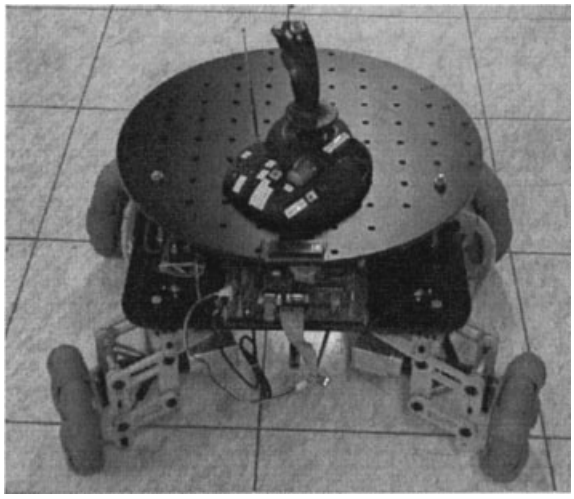

Figure 16. Photo of OMR-SOW.

gradability can be improved with the extended operating regions in that smaller motors can be used to meet the given performance specifications. For example, let T_1 be the torque required to meet the specification. It is clear that this torque cannot be obtained by use of the speed reducer alone since the operating region is limited to region II. One way to obtain this torque is to use the larger motor combined with a speed reducer, which extends the operating region to region IV (*a-c-g-h-j-a*). Addition of the CVT, however, enables the torque T_1 to be available even with the smaller motor combined with the speed reducer belonging to region II. It is noted that the size of a motor can be made smaller with the increased range of transmission ratio of the CVT, which justifies the proposed mechanism which can substantially increase the range of transmission ratio.

Referring to Figures 11 and 14, when the steering range is $-17.5°–+17.5°$ in the variable footprint mechanism,[9,10] the ranges of the translational velocity ratio and force ratios are 0.56–1.08 and 1.79–0.925, respectively, thereby resulting in the ratio of 1.93 (i.e., 1.08/0.56 or 1.79/0.925). On the other hand, when the steering range extends to $-30°–+30°$ in the proposed mechanism, the ranges of the translational velocity ratio and force ratios are extended to 0.52–1.93 and 1.93–0.52, respectively, thereby resulting in the ratio of 3.71 (i.e., 1.93/0.52). An increase in the steering range by an angle of 12.5° can yield an increase in the robot performance by a factor of 1.93, which justifies the advantage of the proposed mechanism.

4. EXPERIMENTS AND DISCUSSIONS

4.1. Construction of OMR-SOW

An omnidirectional mobile robot with the proposed variable wheel arrangement mechanism was designed and constructed as shown in Figure 16. This robot contains four wheel modules comprising the omnidirectional wheel connected to each motor, a synchronous steering mechanism, and a square platform whose side is 500 mm. The height of the platform from the ground is 420 mm, and the motor drives and controller are placed in this space between the platform and ground. The robot can be used as a wheelchair since it is designed to have a payload of more than 100 kg. Table I summarizes specifications of the OMR-SOW.

A synchronous steering mechanism shown in Figure 17(a) constrains four steerable omnidirectional wheels to rotate for steering with a single DOF. A linear guide and links are used in this mechanism for synchronous motion. Four wheel modules are steered at each steering axis and all modules are interconnected by the synchronous steering mechanism. A wheel module shown in Figure 17(b) consists of a motor module, an omnidirectional wheel, pulleys, a timing belt, and a suspension system. The motor module is composed of a motor (MAXON, 150 W, 24 V), a

Table I. Specifications of OMR-SOW.

Feature		Specifications
Weight		49.2 kg
Width	Min.	66 cm
	Max.	78 cm
Length	Min.	66 cm
	Max.	78 cm
Height		42 cm
Battery	For logic	12 V, 7 AH
	For motor	24 V, 10 AH
Payload		100 kg
Radius of wheel: R		10 cm
Steering axis from c.g.: L_0		28.3 cm
Steering length: l		14.2 cm
Range of steering angle		–30°–30°
Reduction ratio of CVT		0.517–1.93

reduction gear (26:1), an encoder, and a brake. Since the reduction ratio by the pulley is 3:1, the total reduction ratio is 78:1. The wheel velocity is measured by an encoder integrated in the motor. The suspension system, composed of a 4 bar linkage, a damper, and a spring, is required to ensure that all wheels are in contact with the ground at all times, which is very important in this type of four-wheeled mechanism. This suspension can also absorb the shock transmitted to the wheels.

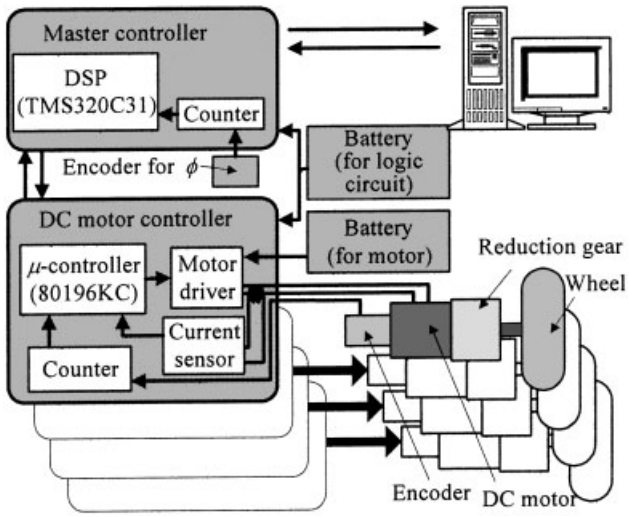

Figure 18. Control systems for OMR-SOW.

Figure 18 illustrates the control systems for the mobile robot. DSP (TMS320C31) is used as a master controller, while the microcontroller 80196KC is employed as a motor controller. The mobile robot can move autonomously, but the PC is used to monitor the whole system and collect data. The master controller plans the robot trajectory and commands the appropriate signal depending on the type of operation (i.e., speed mode or torque mode) to the motor drives where motor control is performed.

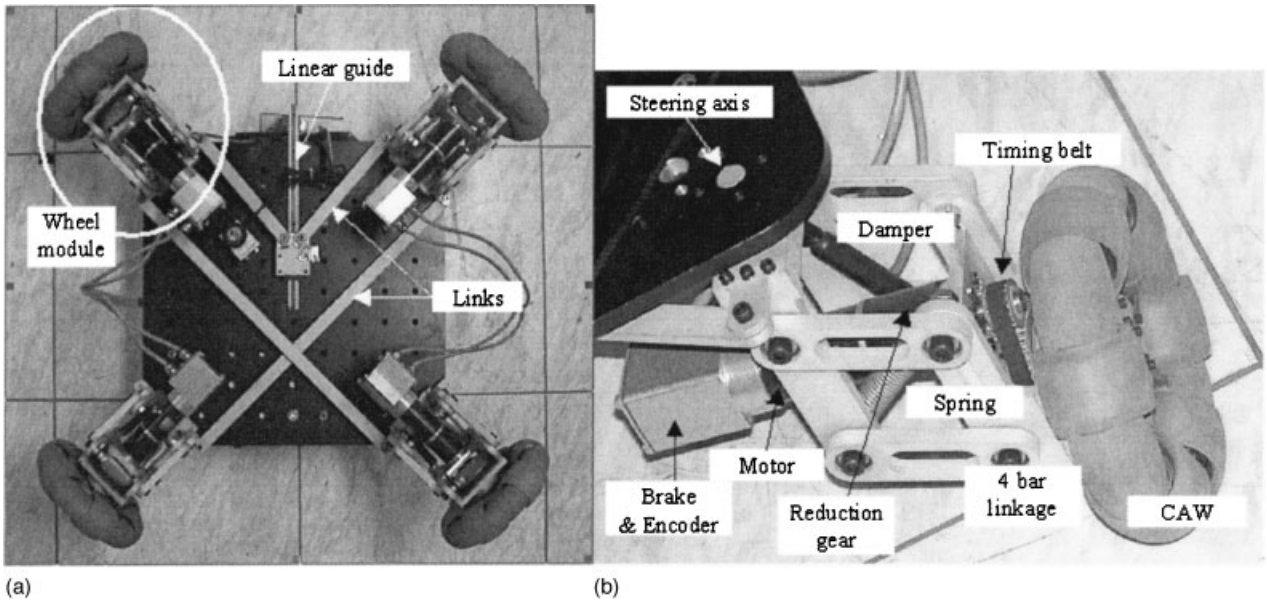

Figure 17. Structure of (a) synchronous steering mechanism and (b) omnidirectional wheel module.

4.2. Motion Control

The motion of a mobile robot can be controlled by wheel velocities. As explained in Section 3, the relationship between the robot velocity and the wheel velocities is given by Eq. (11) Therefore, when the desired robot motion is given, the reference velocity of each wheel can be computed by

$$\mathbf{V}_{w,ref}=\mathbf{J}^{-1}\mathbf{V}_{r,ref}, \tag{36a}$$

$$[v_{1ref} \quad v_{2ref} \quad v_{3ref} \quad v_{4ref}]^T = \mathbf{J}[v_{xref} \quad v_{yref} \quad \dot{\psi}_{ref} \quad \dot{\phi}_{ref}]^T. \tag{36b}$$

If each wheel is controlled to follow the reference velocity, then a robot can achieve the desired motion. Suppose that there is no slip between the wheel and the ground. The wheel velocity is represented by the angular velocity of a wheel and the radius of an omnidirectional wheel:

$$\mathbf{V}_w=[v_1 \quad v_2 \quad v_3 \quad v_4]^T=R\cdot[\omega_1 \quad \omega_2 \quad \omega_3 \quad \omega_4]^T. \tag{37}$$

Control of wheel velocity (thus the angular velocity of a wheel) can be performed by motor control. In this paper, the wheel velocity is controlled to follow the reference velocity profile by a PI controller.

Practically, all mobile robots have slip between the wheels and the ground to some extent. This slip causes the real motion to be different from the desired one. The wheel velocity can be obtained by the wheel angular velocity in the no slip condition, but this is not the case when slip exists. However, the velocity transmitted to the robot body by the wheel will still be called the wheel velocity even when slip arises. Suppose that the wheel velocity vector with slip is given by

$$\hat{\mathbf{V}}_w=[\hat{v}_1 \quad \hat{v}_2 \quad \hat{v}_3 \quad \hat{v}_4]^T. \tag{38}$$

Then, the difference between the wheel velocity with no slip and that with slip is represented by

$$\tilde{\mathbf{V}}_w=\mathbf{V}_w-\hat{\mathbf{V}}_w. \tag{39}$$

The difference of the robot velocity by slip is given from Eq. (11) as follows:

$$\tilde{\mathbf{V}}_r=\mathbf{V}_r-\hat{\mathbf{V}}_r=\mathbf{J}\tilde{\mathbf{V}}_w. \tag{40}$$

If an additional sensor (e.g., a gyroscope, a vision system, a laser range finder) measures robot motion, this error can be compensated for. Control for steering of the OMR-SOW when slip arises is discussed below.

If the steering angle is changed, the Jacobian of the OMR-SOW is also changed. Since the Jacobian affects all motions of the robot, the steering angle ought to be controlled accurately. In the case that there is a slip, measurement of the steering angle is needed to accurately control the angle. To measure a steering angle, an optical encoder is installed at the steering axis. In Eq. (40), the difference in steering angle by the slip is obtained by

$$\tilde{\dot{\phi}}=\dot{\phi}_{ref}-\dot{\phi}=\frac{1}{4l}(-\tilde{v}_1+\tilde{v}_2-\tilde{v}_3+\tilde{v}_4). \tag{41}$$

The integration of this value is the error of steering angle. The reference steering velocity $\dot{\phi}_{ref}$ can be obtained by the difference between the reference steering angle ϕ_{ref} and the steering angle ϕ measured by the encoder as follows:

$$\dot{\phi}_{ref}=K_\phi(\phi_{ref}-\phi), \tag{42}$$

where K_ϕ is the control gain of steering. If the reference steering angle is larger than the measured steering angle, the reference steering velocity has plus sign. The steering angle can follow the reference steering angle by proper control. Figure 19 shows the control system with compensation for a steering angle.

4.3. Experiments of OMR-SOW

Some performance tests for the prototype vehicle have been conducted. Tracking performance of the vehicle with one person on it has been tested for various trajectories. Figure 20 shows experimental results for a square trajectory. The vehicle control algorithm generates the required vehicle velocity and then computes the velocity of each wheel to achieve the desired motion through the Jacobian analysis given in Eq. (11). In Figure 20(a), the solid line represents the actual trajectory of the robot and the dashed line is the reference trajectory. Triangles in the figure represent the position and orientation of the robot in every second and the triangle filled with gray color is the start location. Figure 20(b) shows robot velocity and steering angle. The robot velocity follows the reference input faithfully. Since the accumulated position

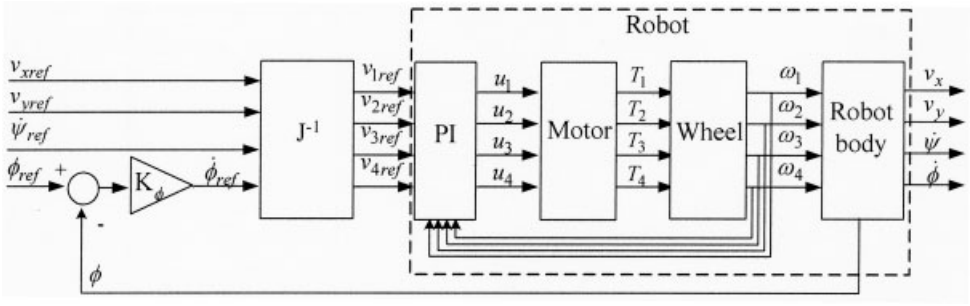

Figure 19. Control structure with compensation for steering angle.

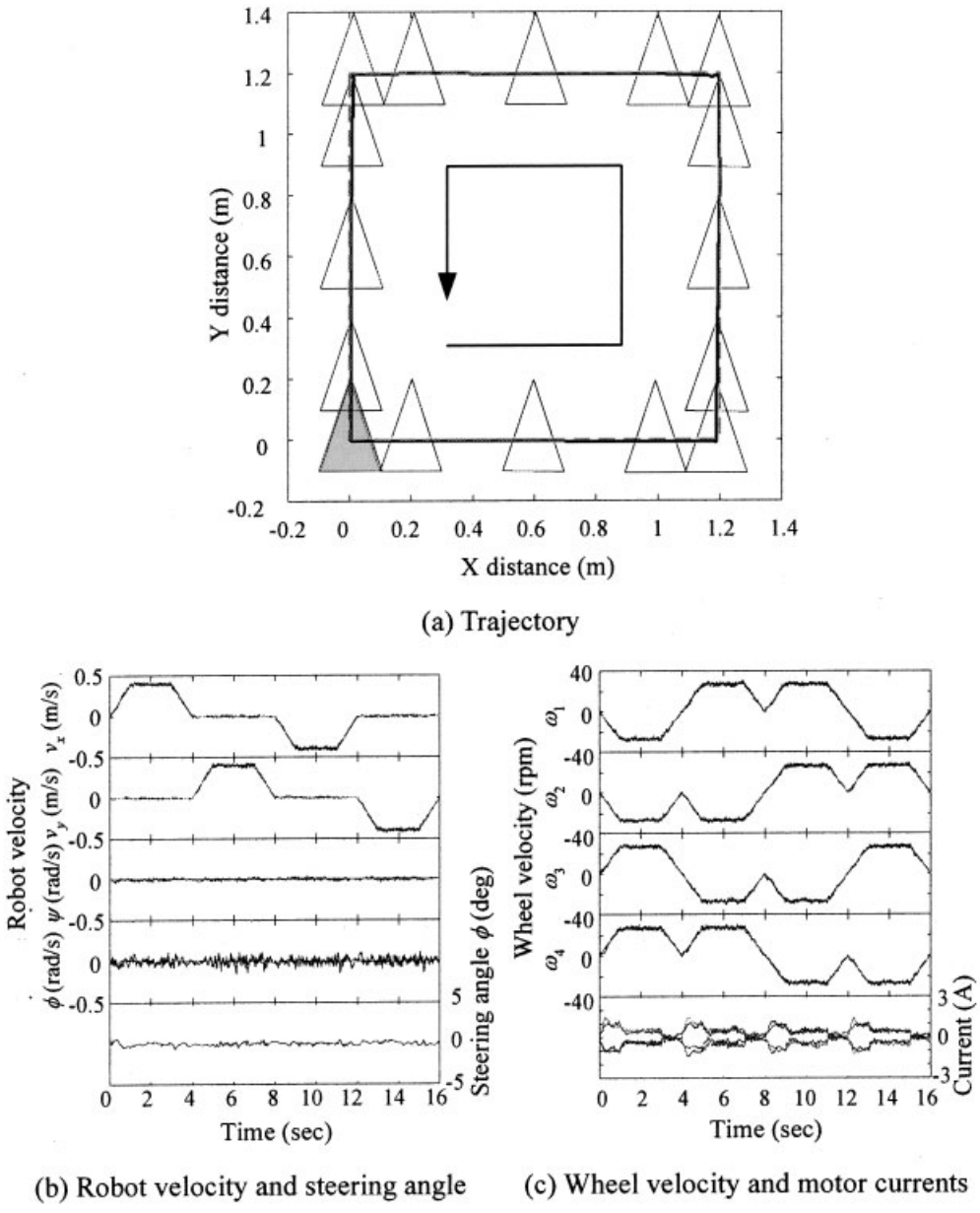

Figure 20. Experimental results of tracking performance for a rectangular trajectory.

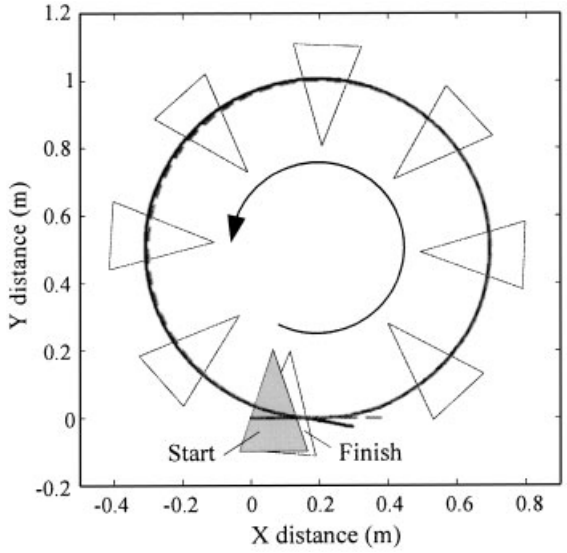

Figure 21. Experimental results of tracking performance for a circular trajectory (solid line: actual trajectory, dashed line: reference trajectory).

error is not compensated for, however, there exists a position error between the reference and actual trajectory. Figure 20(c) shows each wheel velocity and motor currents.

Experiments of Figure 20 are associated with only translational motions. However, Figure 21 showing tracking performance for a circular trajectory is associated with both translational and rotational motion. In the experiment, the robot moves in the x-direction and simultaneously rotates about the z-axis. It is seen that the actual trajectory represented in the solid line tracks the reference reasonably relatively well. Some error is observed around the finish since the prototype vehicle does not implement any position control algorithm for this test and thus the position error has been accumulated during motion.

Figure 22 shows experimental results for a CVT function. Note that the robot moves only in the x direction in the figure. All four wheels of the robot are controlled to have an identical and fixed rotational speed (i.e., 25 rpm). As the steering angle decreases, the robot velocity increases despite fixed wheel velocities. It is noted that the velocity and force ratios change with the steering angle as well. This means that the OMR-SOW can function as a CVT.

5. CONCLUSIONS

In this research, an omnidirectional mobile robot with steerable omnidirectional wheels (OMR-SOW) has been proposed and the kinematic and dynamic analysis of a proposed robot has been conducted. The motion control system of a robot was developed and various experiments were conducted. As a result of this research, the following conclusions are drawn.

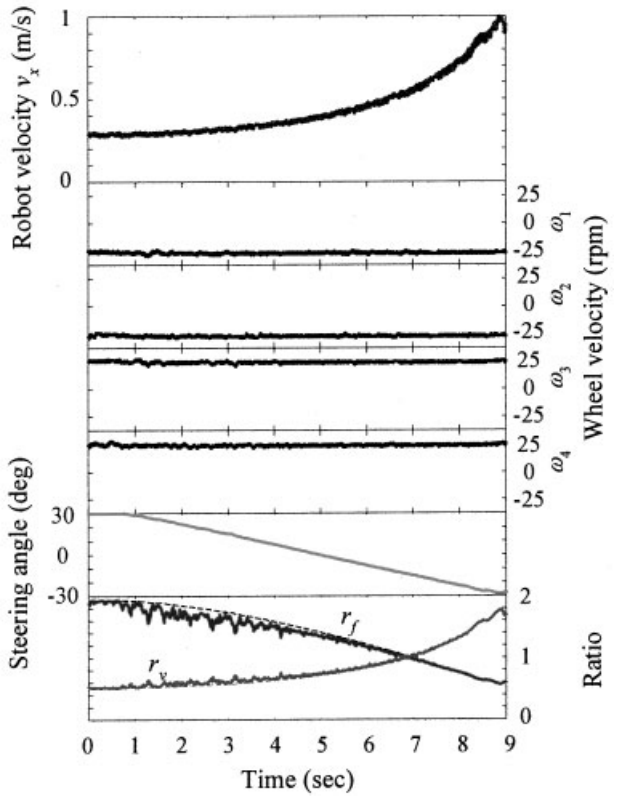

Figure 22. Experimental results showing increasing robot velocity for fixed wheel velocities by adjusting steering angle.

1. In the OMR-SOW the wheel modules rotate for steering about the corners of the robot body, thus providing good tipping stability independent of wheel arrangements.
2. The OMR-SOW has 4 DOFs which consist of 3 DOFs for omnidirectional motion and 1 DOF for steering. This steering DOF functions as a continuously variable transmission (CVT). Therefore, the OMR-SOW can be also considered as an omnidirectional mobile robot with CVT.
3. The steering range has been significantly increased, which leads to an increase in the velocity ratio from the wheel velocity to the robot velocity. Due to this feature, the size of an actuator to meet the specified performance can

be reduced or performance of the mobile robot such as gradability can be enhanced for given actuators.

One of the most important features of the OMR-SOW is the CVT function which can provide energy efficient drive of a robot. If the CVT is not properly controlled, however, energy efficiency capability can be deteriorated. Hence, research on the proper control algorithm is under way for energy efficient drive.

REFERENCES

1. J.F. Blumrich, Omnidirectional vehicle, United States Patent 3,789,947, 1974.
2. B.E. Ilou, Wheels for a course stable self-propelling vehicle movable in any desired direction on the ground or some other base, United States Patent 3,876,255, 1975.
3. M. West and H. Asada, Design of ball wheel mechanisms for omnidirectional vehicles with full mobility and invariant kinematics, J Mech Des (1997), 119–161.
4. M. Wada and S. Mory, Holonomic and omnidirectional vehicle with conventional tires, Proc of IEEE Int Conf on Robotics and Automation, 1996, pp. 3671–3676.
5. B. Carlisle, An omnidirectional mobile robot, Development in robotics, Kempston, 1983, pp. 79–87.
6. F. Pin and S. Killough, A new family of omnidirectional and holonomic wheeled platforms for mobile robot, IEEE Trans Robot Autom 15:(6) (1999), 978–989.
7. P. Muir and C. Neuman, Kinematic modeling of wheeled mobile robots, J Robot Syst 4:(2) (1987), 281–340.
8. H. Asama, M. Sato, L. Bogoni, H. Kaetsu, A. Masumoto, and I. Endo, Development of an omnidirectional mobile robot with 3 DOF decoupling drive mechanism, Proc of IEEE Int Conf on Robotics and Automation, 1995, pp. 1925–1930.
9. M. Wada and H. Asada, Design and control of a variable footprint mechanism for holonomic omnidirectional vehicles and its application to wheelchairs, IEEE Trans Robot Autom 15:(6) (1999), 978–989.
10. K. Tahboub and H. Asada, Dynamic analysis and control of a holonomic vehicle with continuously variable transmission, Proc of IEEE Int Conf on Robotics and Automation, 2000, pp. 2466–2472.
11. K.-S. Byun and J.-B. Song, Design and construction of continuous alternate wheels for an omnidirectional mobile robot, J Robot Syst 20:(9) (2003), 569–579.
12. G. Campion, G. Bastin, and B. D'Andrea-Novel, Structural properties and classification of kinematic and dynamic models of wheeled mobile robot, IEEE Trans Robot Autom 12:(1) (1996), 47–62.